Interaction of Metal Ions with the Antihyperuricemic Drug Allopurinol (H_2L): Synthesis and Crystal Structure of Dimeric $[Zn_2(\mu\text{-}HL)_2Cl_2(H_2O)_2]$†

Gaby Hänggi, Helmut Schmalle and Erich Dubler*
Institute of Inorganic Chemistry, University of Zürich, Winterthurerstrasse 190, CH-8057 Zürich, Switzerland

The complex $Zn^{II}(HL)Cl(H_2O)$ (H_2L = allopurinol = 1,5-dihydropyrazolo[3,4-*d*]pyrimidin-4-one) has been crystallized from aqueous solution. Crystal data: triclinic, space group $P\bar{1}$ (no. 2), a = 7.052(2), b = 7.726(2), c = 8.341(4) Å, α = 69.78(3), β = 87.75(3), γ = 68.27(3)° and Z = 2. The complex exhibits a new centrosymmetric dimeric structure of the type $[Zn_2(\mu\text{-}HL)_2Cl_2(H_2O)_2]$. Two zinc ions with an intramolecular metal-to-metal distance of 3.713(2) Å are bridged by two N(8)–N(9)-chelating anionic allopurinol ligands. The dimeric complex units are stabilized by an extended network of hydrogen bonding contacts. The co-ordinating allopurinol rings are stacked with a mean spacing distance of 3.39 Å. A review of the co-ordinating properties of neutral, anionic and cationic allopurinol including recent crystallographic data is given.

The co-ordinating properties of the oxopurines hypoxanthine (1,7-dihydropurin-6-one) and its 8-aza-7-deaza-derivative allopurinol (1,5-dihydropyrazolo[3,4-*d*]pyrimidin-4-one) are of biochemical interest, since they are substrates of the molybdenum- and iron-containing enzyme xanthine oxidase (xanthine = 3,7-dihydropurine-2,6-dione). Hypoxanthine is oxidized *via* xanthine to uric acid [7,9-dihydro-3*H*-purine-2,6,8-trione], which is subsequently released from the active site of the enzyme.[1] Allopurinol is known to be a potent inhibitor of xanthine oxidase and is used for the treatment of gout. Alloxanthine{1,7-dihydropyrazolo[3,4-*d*]pyrimidine-4,6-dione}, the enzymatic oxidation product of the drug allopurinol, is believed to inhibit uric acid formation by irreversible co-ordination to the reduced form of the molybdenum centre of the enzyme.[2] Differences in the metal-binding pattern of these oxopurines have been suggested to be of significance to their distinctive mode of action during the catalytic turnover.[3]

Crystallographic data of metal complexes of hypoxanthine[4] and of xanthine[5] have recently been reviewed. Much fewer structural data are available on the pyrazolopyrimidine allopurinol. As part of a research program on the co-ordination properties of oxopurines and pyrazolopyrimidines, we describe here a new dimeric zinc complex including two N(8)–N(9)-bridging anionic allopurinol ligands.

Experimental

Synthesis.—Single crystals of $Zn(HL)Cl(H_2O)$ (H_2L = allopurinol) were synthesized by heating a mixture of allopurinol (25 mg, 0.18 mmol) and $ZnCl_2$ (0.040 g, 29.4 mmol) in H_2O (30 cm^3) until complete solubilization was observed. The mixture was kept for crystallization at 75 °C. Two weeks later, colourless distorted prismatic crystals (Found: C, 23.95; H, 2.00; Cl, 14.25; N, 22.10. Calc. for $C_5H_5ClN_4O_2Zn$: C, 23.60; H, 2.00; Cl, 13.95; N, 22.05%) were isolated.

Thermal Analysis.—Thermogravimetric data were recorded on a Perkin Elmer thermobalance TGS-2 in a flowing oxygen atmosphere. The thermal decomposition of $Zn(HL)Cl(H_2O)$ (Fig. 1) occurs in a pronounced two-step reaction. Dehydration, starting at a temperature of about 200 °C reveals an anhydrate phase, which is stable in the temperature range 280–350 °C. The observed decrease in weight during the first decomposition step (7.6%) is in accordance with the values calculated for the loss of one water molecule per formula unit (7.1%). The anhydrous zinc complex is decomposed in the temperature range 350–680 °C to ZnO, as evidenced by X-ray powder diffractometry.[6]

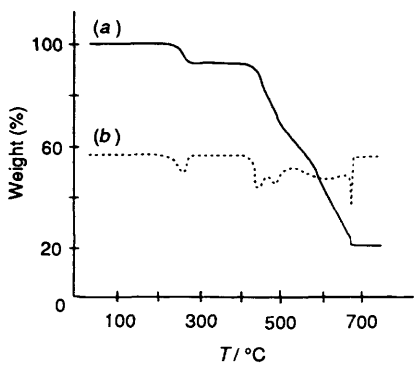

Fig. 1 Thermogravimetric (*a*) and differential thermogravimetric (*b*) curves for the thermal degradation of $Zn(HL)Cl(H_2O)$

Crystallographic Determination.—A transparent, prismatic single crystal was selected for X-ray investigation on an Enraf–Nonius CAD-4 diffractometer with graphite-monochromatized Mo-Kα radiation. Cell parameters were obtained from least-squares refinement of 25 carefully centred reflections in the interval $3.0 < \theta < 13.0°$. Intensity data were collected at room temperature. Three standard reflections checked every 3 h during data collection showed no significant decrease in intensity. Orientation was controlled using four standard reflections at an interval of every 250 reflections. The data were corrected for Lorentz and polarization effects, and a numerical absorption correction, based on ten carefully indexed crystal

† *Supplementary data available:* see Instructions for Authors, *J. Chem. Soc., Dalton Trans.*, 1993, Issue 1, pp. xxiii–xxviii.

Table 1 Crystal data and structure determination parameters of Zn(HL)Cl(H_2O)

Formula	$C_5H_5ClN_4O_2Zn$
M	253.95
Crystal system	Triclinic
Space group	$P\bar{1}$ (no. 2)
a/Å	7.052(2)
b/Å	7.726(2)
c/Å	8.341(4)
α/°	69.78(3)
β/°	87.75(3)
γ/°	68.27(3)
U/Å^3	394.1(3)
Z	2
D_c/g cm^{-3}	2.14
D_m/g cm^{-3}	2.14
Crystal size/mm	0.24 × 0.18 × 0.18
μ/cm^{-1}	32.95
Transmission coefficient (minimum, maximum)	0.540, 0.659
2θ/°	2–60
h, k, l ranges	−9 to 9, −10 to 10, −11 to 11
Scan method	ω–2θ
Scan speed/° min^{-1}	1.8–5.5
Maximum counting time/s	50
No. of reflections measured (including standards)	4563
R_{av} no. of reflections averaged	0.028, 4269
No. of unique reflections	2148
Reflections with $I \geqslant 3\sigma(I)$	1673
No. of variables	138
Largest shift/esd (non-hydrogen parameters)	0.016
$R(F_o)$*	0.063
$R'(F_o)$*	0.074

* $R = \Sigma\|\|F_o\| - \|F_c\|\|/\Sigma\|F_o\|$, $R' = [\Sigma w(\|F_o\| - \|F_c\|)^2/\Sigma w|F_o|^2]^{\frac{1}{2}}$.

Table 2 Positional parameters of Zn(HL)Cl(H_2O)

Atom	x	y	z
Zn	0.516 4(1)	0.581 56(9)	0.264 58(8)
Cl	0.708 9(3)	0.682 7(2)	0.069 6(2)
N(1)	0.904 2(9)	−0.214 5(7)	0.367 2(7)
C(2)	0.862 1(10)	−0.041 8(9)	0.230 9(8)
N(3)	0.770 3(8)	0.135 4(7)	0.232 1(6)
C(4)	0.717 3(8)	0.137 5(7)	0.390 3(7)
C(5)	0.751 5(9)	−0.031 5(7)	0.537 6(7)
C(6)	0.847 6(9)	−0.225 7(8)	0.527 5(7)
O(6)	0.879 2(8)	−0.386 7(6)	0.642 4(6)
C(7)	0.669 1(10)	0.045 8(8)	0.663 2(7)
N(8)	0.592 3(8)	0.243 4(7)	0.597 6(6)
N(9)	0.622 0(8)	0.302 3(6)	0.425 9(6)
O(1)	0.266 7(8)	0.634 1(7)	0.117 7(6)
H(1)	0.960(12)	−0.302(13)	0.354(10)
H(2)	0.890(11)	−0.057(10)	0.137(9)
H(7)	0.644(15)	0.006(15)	0.755(13)
H(11)	0.276(12)	0.675(12)	0.007 8(10)
H(12)	0.220(14)	0.575(13)	0.127(11)

faces, was applied. The structure was solved by Patterson synthesis using the program SHELXS 86[7] and refined with full-matrix least-squares and successive Fourier difference calculations applying SHELX 76.[8] After anisotropic refinement of the non-hydrogen atoms all hydrogen atoms could be localized in the Fourier difference maps and were included in the refinement with free positional and free isotropic thermal parameters. The final refinement minimizing $\Sigma w(\|F_o\| - \|F_c\|)^2$ with $w = 1/[\sigma^2(F_o) + 0.0005F_o^2]$, converged to $R = 0.063$ and $R' = 0.074$ respectively. Maximum and minimum residual electron densities in the final Fourier difference synthesis were 2.27 e Å^{-3}, located at a distance of 0.89 Å from Zn, and −1.92 e Å^{-3},

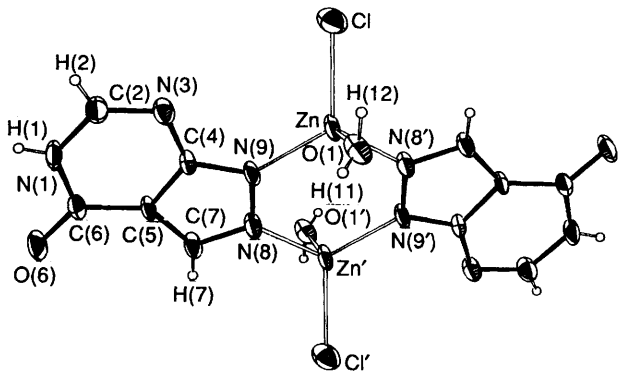

Fig. 2 ORTEP[10] drawing of the dimeric unit in Zn(HL)Cl(H_2O); the thermal ellipsoids shown are drawn at the 50% probability level

Table 3 Interatomic bond distances (Å) and angles (°) of Zn(HL)Cl(H_2O)

Zn–N(8')	1.994(6)	C(5)–C(6)	1.431(8)
Zn–N(9)	1.976(4)	C(6)–N(1)	1.364(8)
Zn–Cl(1)	2.198(2)	C(5)–C(7)	1.385(9)
Zn–O(1)	2.015(6)	C(7)–N(8)	1.326(7)
Zn · · · Zn	3.713(2)	N(8)–N(9)	1.377(7)
N(1)–C(2)	1.358(7)	N(9)–C(4)	1.332(8)
C(2)–N(3)	1.283(8)	C(6)–O(6)	1.226(6)
N(3)–C(4)	1.361(8)	N(3)–N(9)	2.383(8)
C(4)–C(5)	1.397(6)		
N(8')–Zn–N(9)	107.6(2)	N(9)–Zn–Cl(1)	119.4(2)
N(8')–Zn–Cl(1)	113.3(2)	N(9)–Zn–O(1)	109.7(2)
N(8')–Zn–O(1)	103.8(2)	O(1)–Zn–Cl(1)	101.7(2)
Zn–N(8)–C(7)	141.3(4)	Zn–N(9)–C(4)	127.9(4)
Zn–N(8)–N(9)	127.0(4)	Zn–N(9)–N(8)	124.6(4)
C(6)–N(1)–C(2)	124.6(6)	C(7)–N(8)–N(9)	108.4(5)
N(1)–C(2)–N(3)	126.4(6)	N(8)–N(9)–C(4)	107.3(4)
C(2)–N(3)–C(4)	112.7(5)	N(9)–C(4)–C(5)	110.2(5)
N(3)–C(4)–C(5)	125.3(5)	N(3)–C(4)–N(9)	124.5(4)
C(4)–C(5)–C(6)	119.7(5)	C(6)–C(5)–C(7)	136.4(5)
C(5)–C(6)–N(1)	111.3(5)	N(1)–C(6)–O(6)	121.3(6)
C(4)–C(5)–C(7)	103.9(5)	C(5)–C(6)–O(6)	127.4(6)
C(5)–C(7)–N(8)	110.2(5)		

located 0.93 from Zn and 1.40 Å from N(9). Atomic scattering factors for the neutral atoms and anomalous dispersion terms for C, H, N, O and S were those in SHELX 76 and for Zn they were taken from ref. 9. All calculations were performed on a HDS AS/XL V60 computer. Crystal parameters, details of data collection and results of the refinement are summarized in Table 1 and the refined atomic parameters are listed in Table 2.

Additional material available from the Cambridge Crystallographic Data Centre comprises thermal parameters.

Discussion

Molecular Structure.—The zinc complex described here represents the first structurally-characterized metal complex involving the bridging of two metal atoms by an allopurinol ligand. The structure consists of molecular centrosymmetric units of the type $[Zn_2(\mu\text{-HL})_2Cl_2(H_2O)_2]$ (Fig. 2). Two zinc ions, separated by an intramolecular metal-to-metal distance of 3.713(2) Å, are bridged by two N(8)–N(9)-chelating anionic allopurinol ligands. The remaining two co-ordination sites of each zinc ion are occupied by a chloride ion and by a water molecule. The resulting ZnN_2ClO tetrahedron with bonding angles 101.7(2)–119.4(2)° is markedly distorted. The distortion probably is a consequence of the constraints induced by the bridging ligand. Interatomic bonding distances and angles are summarized in Table 3. The zinc ions are displaced +0.164 and −0.164 Å from the plane defined by the four-co-ordinating

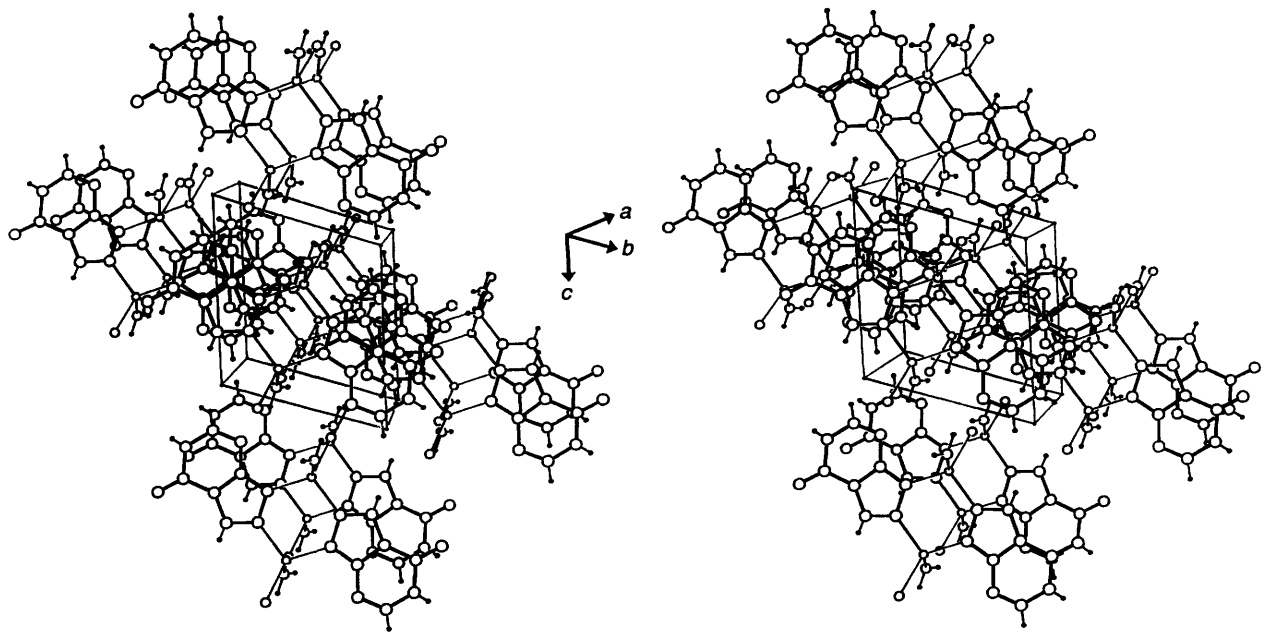

Fig. 3 ORTEP[10] drawing of the packing diagram of $Zn(HL)Cl(H_2O)$

Table 4 Co-ordination and protonation sites of allopurinol (H_2L)

Compound	Structure	Co-ordination	Protonation	Reference
H_2L		—	N(1), N(9)	17
$[H_3L]Cl$		—	N(1), N(3), N(8)	16
$[M^{II}(H_2L)_2(SO_4)(H_2O)_3]\cdot H_2O$ (M = Cu, Co, Ni, Zn or Cd)	**Ia**	Monomeric, N(8)	N(1), N(9)	11 12
$[M^{II}(H_2L)_2Cl_2(H_2O)_2]$ (M = Co or Ni)	**Ib**	Monomeric, N(8)	N(1), N(9)	13
$[Rh^{I}Cl(H_2L)(CO)_2]\cdot MeOH$	**Ic**	Monomeric, N(9)	N(1), N(8)	14
$Zn^{II}(HL)Cl(H_2O)$	**IIa**	Dimeric, N(8), N(9)	N(1)	This work
$(HgMe)_2L\cdot 2H_2O$	**IIb**	N(1), N(9)	—	16
$[\{Cu^{II}(H_3L)Cl_3\}_n]$	**III**	Chlorine-bridged polymeric, N(9)	N(1), N(3), N(8)	15

nitrogen atoms. The plane defined by H_2O–Cl–Zn–Zn′–Cl′–H_2O′ is practically perpendicular (90.5°) to the plane through the four co-ordinating nitrogen atoms. The allopurinol mono-anion has a hydrogen atom attached at the pyrimidine nitrogen atom N(1), but not at N(3), N(8) or N(9). A stereoview of the packing of the dimeric units is given in Fig. 3.

Co-ordinating Properties of Allopurinol and of other Oxopurines.—The pyrazolic nitrogen atom N(8) has been established as the predominant metal-binding site of neutral allopurinol in seven monomeric sulfato- or chloro-complexes.[11–13] Monodentate N(9) co-ordination of neutral allopurinol has only been reported for a rhodium carbonyl compound.[14] Under acidic conditions, monodentate N(9) co-ordination of an allopurinolium cation is observed in the copper complex $[\{Cu^{II}(H_3L)Cl_3\}_n]$, which exhibits a chlorine-bridged polymeric chain structure.[15] Finally two-fold negatively charged allopurinol co-ordinates through N(1) and N(9) to different methyl-mercury cations in $(HgMe)_2L\cdot 2H_2O$.[16] A summary of the co-ordination and protonation sites of neutral, anionic and cationic allopurinol established by X-ray crystallography is shown in Table 4 and Fig. 4 gives a schematic presentation of the respective co-ordination types.

The dimeric structure presented in this paper with the allopurinol N(8)–N(9) bridging is unique among allopurinol complexes. However, the complex $(HgMe)_2L\cdot 2H_2O$ mentioned above represents a closely related structure, if additional weak N(8)-metal interactions are taken into consideration.[16] This complex can also be described as consisting of dimers with the allopurinol N(8)–N(9) bridging, if the N(8)–Hg interaction is believed to be bonding [2.81(1) Å, compared to N(1)–Hg 2.08(1) and N(9)–Hg 2.10(1) Å] (Fig. 4, structure **IIb**). In contrast to allopurinol, the naturally occurring isomer hypoxanthine (L′) forms stable dimers with the general formula $[M_2(\mu\text{-}L')_2(SO_4)_2(\mu\text{-}H_2O)_2(H_2O)_2]$ where M = Cu, Co, Ni, Cd or Zn.[15,18] In these dimeric hypoxanthine complexes, two metal ions are bridged by two neutral N(3)–N(9)-chelating ligands, thus leading to the formation of five-membered rings. In the zinc compound described here, however, anionic allopurinol is bridging by two adjacent atoms, N(8) and N(9) of the pyrazole ring, thereby forming a four-membered ring. A further marked difference between these two structures is evidenced by the fact, that in the hypoxanthine complex the water molecules in addition act as bridging ligands between the two metal ions, whereas terminal water molecules only are found in $[Zn_2(HL)_2Cl_2(H_2O)_2]$.

Protonation versus *Co-ordination.*—There is a distinctive correlation between hydrogen-atom attachment in the free oxopurine base and the site of the metal co-ordination. It has repeatedly been postulated (see, for example, Sheldrick and Bell[16]) that 'metal cations will co-ordinate first to that nitrogen atom of the five-membered ring of purines, which is protonated in the free neutral base.' Our investigations into oxopurines, however, have resulted in the opposite conclusion that the metal cations are predominantly co-ordinating to that nitrogen atom of the five-membered ring, which is *not* bonded to a hydrogen atom in the free neutral base. From the chemist's point of view, this result seems reasonable, because the nitrogen atom, which is not protonated formally bears a

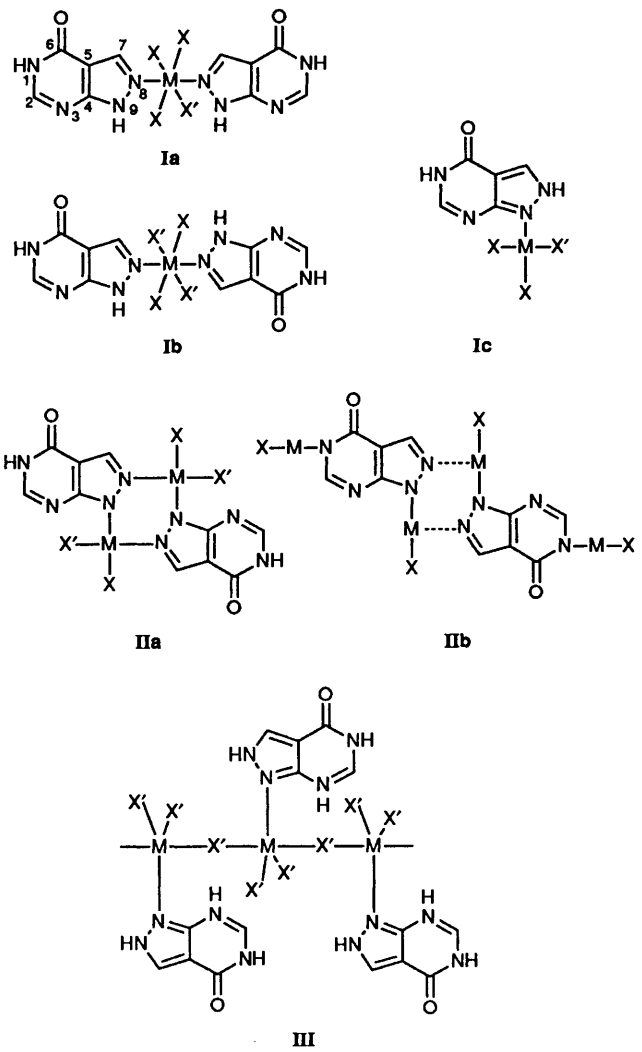

Fig. 4 Schematic presentation of the co-ordinating interaction of neutral (**Ia–Ic**), anionic (**IIa**, **IIb**) and cationic (**III**) allopurinol, as established by X-ray crystallography. **Ia**: M = Cu, Co, Ni, Zn or Cd; X = H_2O; X′ = SO_4; **Ib**: M = Co or Ni, X = H_2O, X′ = Cl; **Ic**: M = Rh, X = CO, X′ = Cl; **IIa**: M = Zn, X = H_2O, X′ = Cl; **IIb**: MX = HgMe; **III**: M = Cu, X′ = Cl

free electron pair immediately available for co-ordination to a metal atom without any rearrangement by tautomerization.

From ^{13}C NMR spectroscopic studies it was concluded that neutral allopurinol is present in aqueous solution as a mixture of 1*H*,9*H*- and 1*H*,8*H*-tautomers.[19] Therefore, according to our rule, co-ordination through N(8) as well as through N(9) has to be expected. However, in the crystal structure of neutral allopurinol the hydrogen atoms are localized at the nitrogen atoms N(1) and N(9), but not at N(8).[17] In accordance with this fact, in seven out of eight structurally-characterized complexes containing neutral allopurinol as a monodentate ligand metal binding through N(8) and not through N(9) has been observed.[11–13] Therefore, the tautomeric forms present in aqueous solution have only minor influence on the co-ordination of neutral allopurinol realized in its crystalline complexes. Metal binding through the sterically less restricted site therefore seems to be an important factor favouring monodentate N(8) co-ordination.

In the allopurinolium cation, the hydrogen atoms are bonded to N(8) of the pyrazole ring and to both nitrogen atoms of the pyrimidine ring.[16] In accordance with the concept formulated above, the nitrogen atom N(9) must be regarded as a potential metal binding site for this molecule. This suggestion is supported by the finding, that in $[\{Cu^{II}(H_3L)Cl_3\}_n]$, the only metal complex of the allopurinolium cation which has been structurally characterized, monodentate co-ordination through N(9) occurs.[15]

Deprotonation of allopurinol occurs at the pyrazolic nitrogen atom and therefore co-ordination of the monoanion can take place at both nitrogen atoms of the pyrazole ring, resulting in the dinuclear zinc complex reported here.

Geometry of Allopurinol.—Changes in the geometry of oxopurines induced by tautomerization, co-ordination or protonation have been elucidated from experimental X-ray data as well as from quantum chemical geometry optimization, using semi-empirical and *ab initio* methods.[20] The major influence on protonation observed for the purine derivative allopurinol is an increase in the corresponding C–N–C angle of about 3–4° accompanied by a reduction in the adjacent angles of approximately 2°. Monodentate co-ordination at N(8) of the pyrazole ring induces changes in the allopurinol geometry similar to, but much smaller than, those effected by protonation.[12]

A corresponding interpretation of the structural changes typical for N(8)–N(9)-bridging allopurinol is difficult since the angles C(7)–N(8)–N(9) and N(8)–N(9)–C(4) are mainly influenced by deprotonation. Deprotonation at N(8) results in a decrease in C(7)–N(8)–N(9) from 113.8(1)° in the allopurinolium cation,[16] where N(8) is protonated, to 108.4(5)° in $[Zn_2(\mu\text{-}HL)_2Cl_2(H_2O)_2]$, where N(8) is co-ordinating to a zinc atom. The bonding angle N(8)–N(9)–C(4) is reduced upon deprotonation at N(9) from 110.7(2)° in neutral 1*H*,9*H*-allopurinol[18] to 107.3(4)° in the zinc complex containing monoanionic 1*H*-allopurinol, and the adjacent angle N(9)–C(4)–C(5) is increased from 107.8(3) to 110.2(5)°. A comparison of the mean ligand geometry of N(8)-co-ordinating 1*H*,9*H*-allopurinol in the sulfato- and chloro-complexes mentioned above with the corresponding values in the N(8)–N(9)-bridging monoanionic allopurinol [C(7)–N(8)–N(9) 106.9(1), 108.4(5); N(8)–N(9)–C(4) 110.6(1), 107.3(4); and N(9)–C(4)–C(5) 107.4(1), 110.2(5)° respectively] again shows that the main differences are observed within the pyrazole ring.

Purine Stacking.—The bridging allopurinol ligands show a small non-planarity with a maximum deviation of 0.026 Å of the atom C(6) from the least-square plane through the nine ring atoms. The respective deviation of the extra-annular oxygen atom O(6) is 0.090 Å.

A packing diagram of the unit cell of $[Zn_2(\mu\text{-}HL)_2Cl_2(H_2O)_2]$ is presented in Fig. 3. An interesting feature of purine compounds is their solid-state stacking pattern, involving partial overlap of the polarizable ring systems. In the dimeric complex described here, a stacking of type **II** occurs,[21] where the bases are arranged on top of each other with their pyrazole moiety pointing in opposite directions. The allopurinol molecules are related by inversion and are infinitely stacked approximately along the *a*-axis of the cell, forming sheets of bases parallel to the *bc* plane. The shortest stacking distance, calculated as the mean distance of individual atoms of one molecule from the least-squares plane through the stacking molecule, is 3.388 Å.

Hydrogen Bonding Contacts.—Bond lengths and angles of hydrogen bonding contacts are listed in Table 5. Two dimeric complex units which are related by a centre of inversion are connected to chains along the *b* axis of the unit cell *via* a pair of N(1)–H(1)···O(6) hydrogen bonding contacts. In addition, the hydrogen atom H(1) is involved in a weak hydrogen bond N(1)–H(1)···Cl, thus leading to a bifurcated hydrogen-bonding system around H(1). Hydrogen bonding interactions involving the water molecule of the type O(1)–H(11)···N(3) and O(1)–H(11)···Cl again reveal a bifurcated hydrogen bonding system around H(11). The hydrogen atom H(12) of the co-ordinating water molecule finally participates in a strong

Table 5 Hydrogen bonding contacts of $Zn(HL)Cl(H_2O)$

X–H···Y	X–H/Å	H···Y/Å	X···Y/Å	X–H···Y/°
N(1)–H(1)···O(6)	0.69(9)	2.23(9)	2.916(7)	169(9)
N(1)–H(1)···Cl	0.69(9)	3.07(10)	3.336(7)	106(7)
O(1)–H(11)···N(3)	0.87(8)	1.98(7)	2.807(6)	158(8)
O(1)–H(12)···O(6)	0.64(12)	2.24(9)	2.715(7)	132(11)
O(1)–H(11)···Cl	0.87(8)	3.01(10)	3.283(7)	100(7)

hydrogen bond O(1)–H(12)···O(6) with an O···O distance of 2.715(7) Å.

Acknowledgements

Research grants from the Swiss National Science Foundation (No. 21-27924.89) are gratefully acknowledged.

References

1 R. Hille and V. Massey, in *Metal Ions in Biology*, ed. T. G. Spiro, Wiley, New York, 1985, vol. 7, p. 443.
2 T. R. Hawkes, G. N. George and R. C. Bray, *Biochem. J.*, 1984, **218**, 961.
3 E. J. Stiefel, *Prog. Inorg. Chem.*, 1977, **22**, 1.
4 E. Dubler, G. Hänggi and H. Schmalle, *Inorg. Chem.*, 1990, **29**, 2518.
5 E. Dubler, G. Hänggi and H. Schmalle, *Inorg. Chem.*, 1992, **31**, 3728.
6 Card no. 36-1451, Powder Diffraction File, JCPDS, Swathmore, PA.
7 G. M. Sheldrick, SHELXS 86, in *Crystallographic Computing*, eds. G. M. Sheldrick, C. Krüger and R. Goddard, Oxford University Press, 1985, p. 175.
8 G. M. Sheldrick, SHELX 76, Program for crystal structure determination, University of Cambridge, 1976.
9 *International Tables for X-Ray Crystallography*, Kynoch Press, Birmingham (present distributor Kluwer Academic Publishers, Dordrecht), 1974, vol. 4.
10 C. K. Johnson, ORTEP, Report ORNL-5138, Oak Ridge National Laboratory, TN, 1976.
11 G. Hänggi, H. Schmalle and E. Dubler, *Inorg. Chem.*, 1988, **27**, 3131.
12 G. Hänggi, H. Schmalle and E. Dubler, *Acta Crystallogr., Sect. C*, 1991, **47**, 1609.
13 G. Hänggi, H. Schmalle and E. Dubler, *Acta Crystallogr., Sect. C*, 1988, **44**, 1560.
14 W. S. Sheldrick and B. Günther, *Inorg. Chim. Acta*, 1988, **151**, 237.
15 W. S. Sheldrick and P. Bell, *Z. Naturforsch., Teil B*, 1987, **42**, 195.
16 W. S. Sheldrick and P. Bell, *Inorg. Chim. Acta*, 1987, **137**, 181.
17 F. Bergmann, A. Frank and Z. Neiman, *J. Chem. Soc., Perkin Trans. 1*, 1979, 2795.
18 P. Prusiner and M. Sundaralingam, *Acta Crystallogr., Sect. B*, 1972, **28**, 2148.
19 G. Hänggi, H. Schmalle and E. Dubler, *Acta Crystallogr., Sect. C*, 1992, **48**, 1008.
20 G. Hänggi, Ph.D. Thesis, University of Zürich, Switzerland, 1991.
21 C. E. Bugg, *The Jerusalem Symposia on Quantum Chemistry and Biochemistry*, Jerusalem Academy of Sciences and Humanities, 1972, vol. 4, p. 178.

Received 7th September 1992; *Paper* 2/04802G